Zero: Jurnal Sains, Matematika, dan Terapan

E-ISSN: 2580-5754; P-ISSN: 2580-569X

Volume 9, Number 2, 2025 DOI: 10.30829/zero.v9i2.25849

Page: 443-455



Optimal Control of Cardiovascular Disease Using Pontryagin's Maximum Principle

¹ Arista Fitri Diana



Department of Actuarial Science, Institut Teknologi Statistika dan Bisnis Muhammadiyah Semarang, 50181, Indonesia

² Tarita Intan Soraya

Department of Actuarial Science, Institut Teknologi Statistika dan Bisnis Muhammadiyah Semarang, 50181, Indonesia

³ Mia Siti Khumaeroh



Department of Mathematics, Universitas Islam Negeri Sunan Gunung Djati, Bandung, 40614, Indonesia

⁴ Muhammad Ibnu Hajar



Department of Actuarial Science, Institut Teknologi Statistika dan Bisnis Muhammadiyah Semarang, 50181, Indonesia

Article Info

ABSTRACT

Article history:

Accepted, 20 October 2025

Keywords:

Cardiovascular Disease; Dynamic Model; Hospitalized Compartment; Optimal Control; Pontryagin's Maximum Principle. Cardiovascular disease poses serious global health and economic challenges. This study develops a dynamic model by adapting the infectious-disease SEIR framework to a non-communicable disease context and extending it with a hospitalized compartment. Three control strategies: curative intervention (u_1) , lifestyle modification (u_2) , and preventive screening-education (u_3) are incorporated and optimized using Pontryagin's Maximum Principle. Numerical simulations, calibrated with data from Rinkendiknas, World Health Organization, National Health Insurance program, BMC Public Health, National Library of Medicine, and RS Roemani Muhammadiyah Semarang, show that curative control rapidly reduces early case burden, while lifestyle modification and education sustain long-term declines. With combined controls, the exposed, infected, and hospitalized compartments decrease by 10%, 20,8%, and 7,4%, respectively, while costs are reduced by 28,5% compared to single interventions. The integration of epidemiological models, healthsystem dynamics, and multi-control optimization offers both methodological novelty and practical value for cost-effective cardiovascular disease policy design.

This is an open access article under the CCBY-SA license.



Corresponding Author:

Arista Fitri Diana, Department of Actuarial Science, Institut Teknologi Statistika dan Bisnis Muhammadiyah Semarang Email: aristafitridiana@gmail.com

1. INTRODUCTION

Cardiovascular diseases (CVD) remain the leading cause of death and disability worldwide [1]. The prevalence of CVD rises with age, influenced by non-modifiable factors such as aging and modifiable ones including hypertension, diabetes, dyslipidemia, obesity, smoking, and physical inactivity [2]. In Southeast Asia, rapid urbanization, sedentary lifestyles, and dietary changes have further amplified these risks, underscoring the urgency of early identification and intervention in high-risk groups [3]. Preventive strategies such as regular physical activity, a healthy diet, and early control of risk factors have proven effective in slowing disease progression [4].

Mathematical modeling provides a structured approach to analyze and predict CVD dynamics at the population level [5]. Dynamic compartmental models combined with optimal control theory enable the design of time-dependent interventions that minimize both disease prevalence and associated costs [6]. While SEIR-type models are widely applied to infectious diseases, their adaptation to non-communicable diseases (NCDs) remains limited. Existing CVD models often lack explicit health-system dynamics, such as hospitalization, and rarely incorporate multiple, simultaneous interventions [7].

Pontryagin's Maximum Principle offers a rigorous framework for deriving necessary conditions in optimal control problems [8]. Its applications in infectious diseases have optimized vaccination, treatment schedules, and public health interventions, while in NCDs it has guided management strategies in diabetes [9] and smoking reduction [10]. However, to date, few studies have applied this principle to cardiovascular disease prevention, particularly in Southeast Asian settings where disease burden and health system constraints differ substantially. Santoso et al. [11] emphasized that coordinated cardiovascular care in Indonesia's primary health care system is essential, yet quantitative models to guide such strategies are scarce.

To address this gap, the present study develops an extended SEIHR model for CVD by adapting the SEIR structure commonly used in infectious disease epidemiology and introducing a hospitalized compartment. Three control variables such as, medical intervention, lifestyle modification through physical activity, and preventive screening-education are incorporated and optimized using Pontryagin's Maximum Principle. This combination offers novelty on three fronts: applying an epidemiological modeling framework traditionally used for communicable diseases to a non-communicable condition, integrating hospitalization dynamics that reflect real-world health system pressures, and jointly evaluating three complementary control strategies within the context of Indonesia, using data from Rinkendiknas [12][13], WHO (World Health Organization) [14], National Health Insurance program (BPJS Kesehatan) [15], BMC Public Health [16], National Library of Medicine, and (RS Roemani Muhammadiyah Semarang.

While the model necessarily makes simplifying assumptions (no reinfection, no migration, no recurrent hospitalization), it provides a tractable framework for exploring the effectiveness and cost-efficiency of different intervention strategies. By explicitly linking optimal control to cardiovascular disease dynamics, this study seeks to provide new insights for both mathematical modeling and practical health policy in resource-limited settings.

2. RESEARCH METHOD

This study employs a quantitative approach through the formulation of a dynamic model based on a system of linear differential equations to describe the progression and mitigation dynamics of cardiovascular disease (CVD). The research methodology is divided into five main stages: model formulation, data pre-processing and parameter estimation, stability analysis of the system, optimal control formulation using Pontryagin's Maximum Principle, and numerical simulation with result interpretation.

2.1 Model Formulation

The model formulation was adopted from SEIR model of epidemiology [1], then the model developed based on previous research that modeled cardiovascular disease using an SEIR model [2], which was further extended in this study by incorporating a Hospitalized compartment, representing individuals receiving hospital care, resulting in an SEIHR model. This model consists of five compartments: susceptible individuals (S), exposed individuals (S), infected individuals (S), hospitalized individuals (S), and recovered individuals (S). The following assumptions are made in the formulation of the SEIHR model for cardiovascular disease dynamics:

- a. New individuals enter the susceptible class at a constant rate (λ), and natural death occurs in all compartments at a rate (μ).
- b. Susceptible individuals become exposed due to behavioral or environmental risk factors at a rate (α) and exposed individuals progress to the disease stage at rate (β) .
- c. Infected individuals may be hospitalized (ρ) , recover without hospitalization (σ) , or die naturally (μ) .
- d. Hospitalized individuals may recover (γ)), die due to disease-related complications (θ) , or die naturally (μ) .
- e. Recovered individuals can also experience natural mortality at rate (μ) .

- f. Migration is disregarded since the study assumes a closed population within a specific region and timeframe, where inflow and outflow have minimal impact on disease progression. This aligns with Indonesia's health data framework, which reports statistics within fixed administrative boundaries.
- g. Reinfection or recurrence is excluded due to the chronic and non-communicable nature of CVD and the model's short timescale. Although studies report [17] a 10-year recurrence risk of 30.2% and a lifetime risk of 62.5% for ASCVD patients, the daily recurrence probability is negligible and has minimal impact on model dynamics.

In this study, several simplifying assumptions were applied, including no reinfection, no migration, and no person-to-person transmission to focus on the core progression dynamics, emphasizing transition processes such as exposure, infection, hospitalization, treatment, and recovery. While these assumptions are justifiable for non-communicable diseases (NCDs), such as cardiovascular disease, they inevitably simplify the complexity of real-world dynamics. For instance, recurrent cases may occur in practice, and population inflows from external regions can influence the number of patients in a hospital or community. Acknowledging these limitations, the present model should be viewed as an initial framework that captures the core dynamics of disease progression. Future extensions may incorporate recurrent events and population mobility to improve realism and enhance the robustness of the findings. Then, based on these assumptions, the compartment digram from SEIHR model of cardiovascular as follows.

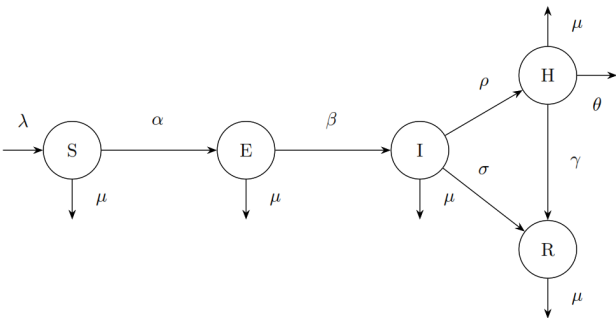


Figure 1. Compartmental Diagram of SEIHR Model

Based on the model proposed by [2], we derive a cardiovascular dynamic model with four compartments: S, E, I, and R. Furthermore, by adopting the infectious disease model [3], which introduces an additional compartment H for hospitalized individuals, the cardiovascular disease model in this study is extended to become the SEIHR model. Thus, the dynamic model of cardiovascular disease can be formulated as follows.

$$\frac{dS}{dt} = \lambda - \alpha S - \mu S$$

$$\frac{dE}{dt} = \alpha S - \beta E - \mu E$$

$$\frac{dI}{dt} = \beta E - (\rho + \mu + \sigma)I$$

$$\frac{dH}{dt} = \rho I - \gamma H - \theta H - \mu H$$

$$\frac{dR}{dt} = \sigma I + \gamma H - \mu R$$
(1)

With the initial conditions $S(0) \ge 0$, $E(0) \ge 0$, $I(0) \ge 0$, $I(0) \ge 0$, $I(0) \ge 0$ and all of the parameters are positive. The explanation of variables and parameters as follows,

Table 1. Description Of Variables

Table 1: Description of Variables				
Notation	Interpretations			
S	Susceptible Individuals			
E	Exposed Individuals			
I	Infected Individuals			
Н	Hospitalized Individuals			
R	Recovered Individuals			

Table 2. Description Of Parameters

Notation	Interpretations		
λ	Annual addition of individuals		
α	Progression rate from susceptible to exposed individuals		
β	Progression rate from exposed to infected individuals		
ho	Progression rate from infected to hospitalized individuals		
σ	Progression rate from infected to recovered individuals		
γ	Progression rate from hospitalized to recovered individuals		
μ	Reduction rate of individuals		
heta	Mortality rate due to cardiovascular disease		

2.2 Sources of Research Data

To construct the SEIHR dynamic model, we utilized patient data collected from RS Roemani Muhammadiyah Semarang during the period 2022-2024. The dataset contains records of both inpatient and outpatient cases of cardiovascular disease, categorized by sex, age group, duration of treatment, and clinical outcome. Although the information is limited to a single hospital and may therefore not capture the full variation of the Indonesian population, the dataset provides rich and detailed clinical information that is particularly valuable for parameter estimation and for illustrating the applicability of the proposed model. The data pre-processing and parameter construction were carried out in the following steps:

In constructing the SEIHR dynamic model, this study relies primarily on secondary data obtained from a range of national and international sources, including Rinkendiknas [12][13], World Health Organization (WHO) [14], National Health Insurance program (BPJS Kesehatan) [15], BMC Public Health [16], National Library of Medicine (NLM) [18], demographic data of national population [19][20][21][22][23][24], national and regional epidemiological surveys on cardiovascular risk factors (e.g., smoking, obesity, hypertension prevalence) [25]. These data sources provide information on the prevalence of cardiovascular disease, hospitalization rates, demographic distributions, length of treatment, and clinical outcomes. By drawing from diverse datasets, the study seeks to capture a more comprehensive picture of cardiovascular disease patterns in Indonesia.

To complement these sources, patient data from Roemani Muhammadiyah Hospital in Semarang are also included, but in a more limited capacity. Rather than serving as the primary basis for parameter estimation, hospital records are used only to establish initial conditions for simulations and to provide clinical-level validation. In this way, the model is grounded in real-world patient data while its key parameters are constructed from broader national and international datasets.

2.3 Stability Analysis

The global stability [26] of the model (2.1) will be analyzed by deriving the exact solution of (2.1). First, analyzed the equillibrium point from model (2.1), we get the solution of (2.1) as follows, $\mathcal{E} = \{S^*, E^*, I^*, H^*, R^*\}$

$$S^* = \frac{\lambda}{\alpha + \mu}$$

$$E^* = \frac{\alpha\lambda}{(\beta + \mu)(\alpha + \mu)}$$

$$I^* = \frac{\beta\alpha\lambda}{(\beta + \mu)(\rho + \mu + \sigma)(\alpha + \mu)}$$

$$H^* = \frac{\beta\alpha\lambda\rho}{(\gamma + \mu + \theta)(\beta + \mu)(\rho + \mu + \sigma)(\alpha + \mu)}$$

$$R^* = \frac{(\rho\gamma + \sigma\gamma + \sigma\mu + \sigma\theta)\beta\alpha\lambda}{(\gamma + \mu + \theta)(\beta + \mu)(\rho + \mu + \sigma)(\alpha + \mu)}$$

Since all parameters are positive, the equilibrium point of model (2.1) is existing. Then we will analyze the stability of model (2.1), we derive the solution of susceptible compartment from the model (2.1) and we get,

$$S(t) = \left(S(0) - \frac{\lambda}{(\alpha + \mu)}\right)e^{-(\alpha + \mu)t} + \frac{\lambda}{(\alpha + \mu)}$$

As $t \to \infty$, we obtain:

$$\lim_{t \to \infty} S(t) = \frac{\lambda}{(\alpha + \mu)} = S^*$$

Thus, the solution S(t) is asymptotically stable to S^* . Then, for the same step we get,

$$E(t) = E(0)e^{-(\beta+\mu)t} + \frac{\alpha}{(\beta-\alpha)} \left(S(0) - \frac{\lambda}{(\alpha+\mu)} \right) \left(e^{-(\alpha+\mu)t} - e^{-(\beta+\mu)t} \right) + \frac{\alpha\lambda}{(\alpha+\mu)(\beta+\mu)} (1 - e^{-(\beta+\mu)t})$$

As $t \to \infty$, we obtain:

$$\lim_{t\to\infty} E(t) = \frac{\alpha\lambda}{(\beta+\mu)(\alpha+\mu)} = E^*$$

The solution E(t) is asymptotically stable to E^* .

Then, similarly the solution of infected compartment, we get,

$$\begin{split} I(t) &= e^{-(\rho + \sigma + \mu)t} I(0) + \frac{\beta E(0)}{(\rho + \sigma + \mu) - (\beta + \mu)} \Big(e^{-(\beta + \mu)t} - e^{-(\rho + \sigma + \mu)t} \Big) \\ &+ \frac{\beta \alpha}{(\beta - \alpha)} \Big(S(0) - \frac{\lambda}{\alpha + \mu} \Big) \Big(\frac{e^{-(\alpha + \mu)t} - e^{-(\rho + \sigma + \mu)t}}{(\rho + \sigma + \mu) - (\alpha + \mu)} - \frac{e^{-(\beta + \mu)t} - e^{-(\rho + \sigma + \mu)t}}{(\rho + \sigma + \mu) - (\beta + \mu)} \Big) \\ &+ \frac{\beta \alpha \lambda}{(\alpha + \mu)(\beta + \mu)} \Big(\frac{1 - e^{-(\rho + \sigma + \mu)t}}{(\rho + \sigma + \mu)} - \frac{e^{-(\beta + \mu)t} - e^{-(\rho + \sigma + \mu)t}}{(\rho + \sigma + \mu) - (\beta + \mu)} \Big) \end{split}$$

As $t \to \infty$, we obtain:

$$\lim_{t\to\infty} I(t) = \frac{\beta\alpha\lambda}{(\beta+\mu)(\rho+\mu+\sigma)(\alpha+\mu)} = I^*$$

The solution I(t) is asymptotically stable to I^* . Next, we use the same step to hospitalized, and recovered compartment, as $t \to \infty$, we obtain H(t), R(t) are asymptotically stable to H^*, R^* . From this analysis, we get that the solution $\mathcal{E} = \{S^*, E^*, I^*, H^*, R^*\}$ are asymptotically stable.

2.4 Optimal Control Analysis

The model (2.1) is modified by incorporating three control functions: curative medical intervention (u_1) , physical activity and healthy lifestyle (u_2) , and screening and preventive education (u_3) . As a result, the model (2.1) becomes:

$$\begin{cases} \frac{dS}{dt} = \lambda - \alpha(1 - u_2 - u_3)S - \mu S \\ \frac{dE}{dt} = \alpha(1 - u_2 - u_3)S - \beta E - \mu E \\ \frac{dI}{dt} = \beta E - (\rho(1 + u_1) + \mu + \sigma)I \\ \frac{dH}{dt} = \rho(1 + u_1)I - \gamma H - \theta H - \mu H \\ \frac{dR}{dt} = \sigma I + \gamma H - \mu R \end{cases}$$

$$(2)$$

Given the initial conditions $S(0) \ge 0$, $E(0) \ge 0$, $I(0) \ge 0$, $H(0) \ge 0$, $R(0) \ge 0$. The explanation of variables and parameters as follows,

Table 3. Description Of Variables

	Tuble of Bescription of Variables				
Notation In		Interpretations			
	S	Susceptible Individuals			
	E	Exposed Individuals			
	I	Infected Individuals			
	Н	Hospitalized Individuals			
	R	Recovered Individuals			

Table 4. Description Of Parameters

Notation	Interpretations
λ	Annual addition of individuals
α	Progression rate from susceptible to exposed individuals
β	Progression rate from exposed to infected individuals
ho	Progression rate from infected to hospitalized individuals
σ	Progression rate from infected to recovered individuals
γ	Progression rate from hospitalized to recovered individuals
μ	Reduction rate of individuals
θ	Mortality rate due to cardiovascular disease

Table 5. Description Of Controls

Notation	Interpretations
u_1	Curative medical intervention control
u_2^-	Physical activity and healthy lifestyle control
u_3	Screening and preventive education control

The objective functional [27] is formulated to optimize the applied control strategies. The goal of the optimal control is to enhance recovery among patients with cardiovascular disease, prevent healthy individuals from progressing to at-risk categories, and increase early detection and public awareness of cardiovascular risk factors [28]. The objective functional [29] of the model (2.2) is defined as follows.

$$J(u_1, u_2, u_3) = \min \int_0^{T_f} \left[A_1 I(t) + A_2 H(t) + \frac{1}{2} \left(B_1 u_1^2(t) + B_2 u_2^2(t) + B_3 u_3^2(t) \right) \right] dt$$
 (3)

Where T_f is the final time, and the coefficients A_1 , A_2 , B_1 , B_2 , B_3 balance the cost factors associated with the scale and importance of the five components of the objective function. To determine the optimal controls (u_1, u_2, u_3) , we use:

$$J(u_1^*, u_2^*, u_3^*) = \min\{J(u_1, u_2, u_3) \mid u_1, u_2, u_3 \in U\}$$

The Hamiltonian function [30] corresponding to equation (2.2) and (2.3) is given as follows.

$$H = A_{1}I(t) + A_{2}H(t) + \frac{1}{2}(B_{1}u_{1}^{2}(t) + B_{2}u_{2}^{2}(t) + B_{3}u_{3}^{2}(t)) + \lambda_{1}\frac{dS}{dt} + \lambda_{2}\frac{dE}{dt} + \lambda_{3}\frac{dI}{dt} + \lambda_{4}\frac{dH}{dt} + \lambda_{5}\frac{dR}{dt}$$

$$H = A_{1}I(t) + A_{2}H(t) + \frac{1}{2}(B_{1}u_{1}^{2}(t) + B_{2}u_{2}^{2}(t) + B_{3}u_{3}^{2}(t)) + \lambda_{1}(\lambda - \alpha(1 - u_{2} - u_{3})S - \mu S) + \lambda_{2}(\alpha(1 - u_{2} - u_{3})S - \beta E - \mu E) + \lambda_{3}(\beta E - (\rho(1 + u_{1}) + \mu + \sigma)I) + \lambda_{4}(\rho(1 + u_{1})I - \gamma H - \theta H - \mu H) + \lambda_{5}(\sigma I + \gamma H - \mu R)$$

$$(4)$$

Theorema 2.1. [31] There exist optimal controls u_1^* , u_2^* , u_3^* and the solution S^* , E^* , I^* , H^* , R^* on system (2.2) that minimize $J(u_1, u_2, u_3)$ on $U = \{u_1, u_2, u_3\}$, when there are adjoint variable $\lambda_1, \lambda_2, \lambda_3, \lambda_4, \lambda_5$ that satisfied:

$$\begin{cases}
-\frac{d\lambda_{1}}{dt} = -\lambda_{1}(\alpha(1 - u_{2} - u_{3}) + \mu) + \lambda_{2}(\alpha(1 - u_{2} - u_{3})) \\
-\frac{d\lambda_{2}}{dt} = -\lambda_{2}(\beta + \mu) + \lambda_{3}\beta \\
-\frac{d\lambda_{3}}{dt} = A_{1} - \lambda_{3}(\rho(1 + u_{1}) + \mu + \sigma) + \lambda_{4}\rho(1 + u_{1}) + \lambda_{5}\sigma \\
-\frac{d\lambda_{4}}{dt} = A_{2} - \lambda_{4}(\gamma + \theta + \mu) + \lambda_{5}\gamma \\
-\frac{d\lambda_{5}}{dt} = -\lambda_{5}\mu
\end{cases}$$
(5)

The transversality conditions at the final time T_f are given by $\lambda_i(T_f) = 0$, i = 1, 2, ..., 5. The optimal controls $(u_1^*(t), u_2^*(t), u_3^*(t))$ are those that minimize the Hamiltonian and satisfy the necessary optimality conditions given by Pontryagin's Maximum Principle [32].

Proof.

We apply Pontryagin's Maximum Principle to obtain the optimal control solutions [33]. The Hamiltonian is differentiated with respect to (u_1, u_2, u_3) , and the optimal control variables are evaluated as follows.

$$\begin{split} \frac{\partial H}{\partial u_1} &= B_1 u_1 + \rho I(\lambda_4 - \lambda_3) \\ \frac{\partial H}{\partial u_2} &= B_2 u_2 + \alpha S(\lambda_1 - \lambda_2) \\ \frac{\partial H}{\partial u_3} &= B_3 u_3 + \alpha S(\lambda_1 - \lambda_2) \end{split}$$

By setting $\frac{\partial H}{\partial u_1} = \frac{\partial H}{\partial u_2} = \frac{\partial H}{\partial u_3} = 0$, the optimal control solutions are obtained as follows.

$$u_{1}^{*} = \begin{cases} 0 & if & \psi_{1}^{*} \leq 0 \\ \psi_{1}^{*} & if & 0 \leq \psi_{1}^{*} \leq 1 \\ 1 & if & \psi_{1}^{*} \geq 1 \end{cases}$$

$$u_{2}^{*} = \begin{cases} 0 & if & \psi_{2}^{*} \leq 0 \\ \psi_{2}^{*} & if & 0 \leq \psi_{2}^{*} \leq 1 \\ 1 & if & \psi_{2}^{*} \geq 1 \end{cases}$$

$$u_{3}^{*} = \begin{cases} 0 & if & \psi_{3}^{*} \leq 0 \\ \psi_{3}^{*} & if & 0 \leq \psi_{3}^{*} \leq 1 \\ 1 & if & \psi_{3}^{*} \geq 1 \end{cases}$$

$$(6)$$

With,

$$\psi_1^* = -\frac{\rho I(\lambda_4 - \lambda_3)}{B_1}$$

$$\psi_2^* = -\frac{\alpha S(\lambda_1 - \lambda_2)}{B_2}$$

$$\psi_3^* = -\frac{\alpha S(\lambda_1 - \lambda_2)}{B_3}$$
(7)

By setting the derivative of the Hamiltonian with respect to the controls equal to zero, the optimal control solutions (u_1^*, u_2^*, u_3^*) from equation (2.6) and (2.7) are obtained, whose values depend on the weighting function ψ_i^* , i = 1,2,3. If $\psi_i^* \leq 0$ the control is not applied, if $\psi_i^* \geq 1$, the control is fully implemented, whereas if $0 < \psi_i^* < 1$ the control is applied partially.

3. RESULT AND ANALYSIS

Numerical simulations compare controlled and uncontrolled models, using parameter estimates and initial values to evaluate the impact of control strategies on disease progression.

3.1 Parameter Estimation

The parameter values used in the SEIHR cardiovascular model were obtained from secondary data sources, including Rinkendiknas [e][f], WHO, BPJS Kesehatan [15], BMC Public Health [16], and the National Library of Medicine (NLM) [18], demographic data of national population [19][20][21][22][23][24]. Among these, the parameters α and β were directly derived from secondary reference data [12][13], while the remaining parameters were estimated through calculations based on secondary data as well [34][35][36][15][16][18][37]. From those sources and calculated, the data were obtained as follows,

Table 6. Value Of Parameters

Tuble 0: Turde 0: Turdineters						
Notation	Value	Unit	References			
λ	11.630	individual	estimated			
μ	0,0077	day ⁻¹	[37][estimated]			
α	0,02716	day ⁻¹	[12]			
β	0,016	day ⁻¹	[13]			
ρ	0,92346	day ⁻¹	[15][estimated]			
γ	0,22814	day ⁻¹	[34][estimated]			
σ	0,1556	day ⁻¹	[34][estimated]			
heta	0,0111	day -1	[34][15][estimated]			

3.2 Sensitivity Analysis

Sensitivity analysis [8] is conducted to assess the robustness of the estimated parameters with respect to small perturbations in the input data. In this study, the sensitivity analysis index is derived from the partial derivative of the equilibrium point with respect to the model parameters. The normalized sensitivity indices are expressed in the form $X_p = \frac{\partial X_i}{\partial p_i} \frac{p_i}{x^{i}}$, where X denotes the compartment at equilibrium state and p represents the parameter [reference]. Specifically, for the infected population, the indices are given by the following equation:

[reference]. Specifically, for the infected population, the indices are given by the following equation:
$$I_{\beta} = \frac{\mu}{(\beta + \mu)}, \quad I_{\alpha} = \frac{\mu}{(\alpha + \mu)}, \quad I_{\lambda} = 1, \quad I_{\rho} = \frac{-\rho}{(\rho + \mu + \sigma)}, \quad I_{\sigma} = \frac{-\sigma}{(\rho + \mu + \sigma)}$$

$$I_{\mu} = -\left(\frac{\mu}{(\beta + \mu)} + \frac{\mu}{(\rho + \mu + \sigma)} + \frac{\mu}{(\alpha + \mu)}\right)$$

Using the data from Table 6, the sensitive index for infected compartment is presented in Figure 2.

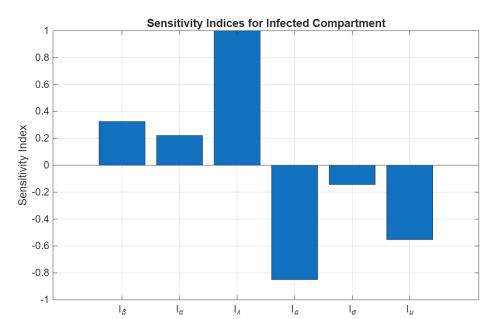


Figure 2. Sensitivity Analysis of infected compartment

The sensitivity analysis shows that the infected compartment is most positively influenced by the recruitment rate (I_{λ} =1), indicating that an increase in λ leads directly to a proportional increase in infection levels. Conversely, the recovery rate (ρ) has the strongest negative effect ($I_{\rho}\approx$ -0.9), meaning that higher recovery substantially reduces infection compartment. The transmission rate (β) and progression rate (α) show moderate positive impacts, while the natural death rate (α) and disease-induced death rate (α) contribute negatively, reducing infection levels. Overall, infection dynamics are most sensitive to recruitment and recovery, with other parameters exerting smaller but notable influences.

Furthermore, the sensitivity analysis results indicate that λ and α are the most influential positive parameters, where an increase in their values leads to a rise in the population across all compartments. In contrast, μ has the strongest negative effect, meaning that increasing its value reduces the population in all compartments. Other parameters, such as β , ρ , γ , σ , and θ , only affect specific compartments according to their respective transition pathways.

3.3 Numerical Simulation

A numerical simulation of the cardiovascular dynamic model was conducted to compare the system's behavior with and without control, to evaluate the effectiveness of combined control strategies, and to estimate the cost savings achieved through the implementation of effective control interventions.

Numerical Simulation of Dynamic Model

From Table 6, the numerical simulation of dynamic model (2.1) with the inisial condition data from RS Roemani Muhammadiyah Semarang S(0) = 701,192, E(0) = 355,935, I(0) = 4.814, H(0) = 207, R(0) = 179, we get the solution graph of the dynamic model (2.1) for the compartments S(t), E(t), I(t), H(t), R(t) at t = 100 days as follows.

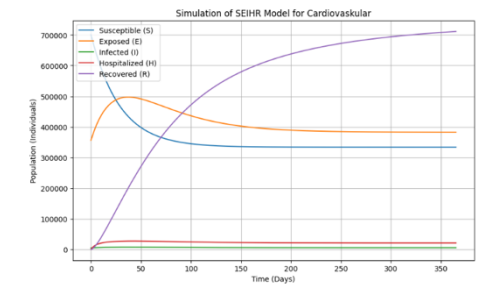


Figure 3. Solution Of Dynamic Model SEIHR Cardiovaskular

Figure 3 presents the one-year SEIHR model simulation for cardiovascular disease. Initially, the susceptible group (S)dominates, reflecting high risk due to unhealthy lifestyles and stress. Over time, this group declines as the exposed population (E)peaks around day 40, marking the critical phase of early disease progression and the need for preventive awareness. The infected (I) and hospitalized (H) groups remain low and stable, consistent with the slow, chronic nature of cardiovascular disease. Meanwhile, the recovered population (R) steadily increases, becoming dominant by year-end, indicating effective natural recovery even without interventions. Overall, the model illustrates a natural shift from susceptibility to recovery, emphasizing the value of early prevention.

Numerical Simulation of Dynamic Model and Control Model

The simulation compares controlled and uncontrolled SEIH models to assess how control strategies reduce cardiovascular disease incidence.

a. Graph of Comparation Susceptible Compartment

In the S(t) compartment, healthy lifestyle control $u_2(t)$ as well as preventive screening and education $u_3(t)$ are applied. The following presents a numerical simulation for the S(t) compartment with and without control.

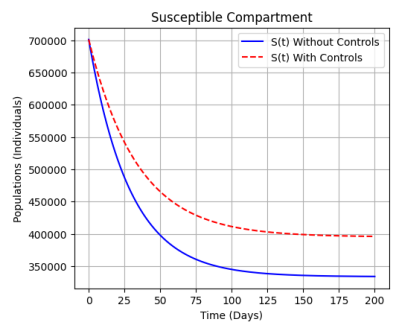


Figure 4. Susceptible Compartment with and without Controls

Figure 4 illustrates the trajectory of the susceptible population S(t) under scenarios with and without control. In the absence of intervention, the number of susceptible individuals declines sharply, eventually stabilizing near 327,000. By contrast, when control measures are applied, the decline occurs more gradually and reaches a higher steady state of around 387,000, the increase is approximately 18,3%. This demonstrates the effectiveness of $u_2(t)$ (healthy lifestyle promotion) and $u_3(t)$ (preventive screening and education) can slow the rate of progression and help preserve a larger portion of the population in a healthier, non-diseased state. In essence, the implementation of control strategies both delays and reduces the transition into advanced stages of cardiovascular risk.

b. Graph Of Comparation Exposed Compartment

In the E(t) compartment, healthy lifestyle control $u_2(t)$ as well as preventive screening and education $u_3(t)$ are applied. The following presents a numerical simulation for the E(t) compartment with and without control.

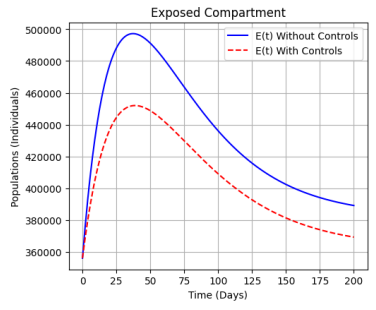


Figure 5. Exposed Compartment with and without Controls

The graph in figure 5 illustrates the dynamics of the exposed population E(t) under two scenarios, with and without control strategies. In the absence of controls, the exposed population rises sharply, reaching a higher peak of nearly 500,000 individuals before gradually declining. This suggests that uncontrolled transmission allows a rapid accumulation of exposed individuals, which prolongs the risk of infection spread. Conversely, when control measures are implemented, the peak of the exposed population is both lower (around 450,000) and reached earlier, the decrease is approximately 10%. Moreover, the decline is steeper, indicating that controls effectively limit the number of individuals at risk and accelerate recovery toward a safer level. Overall, the comparison

highlights the positive impact of interventions: they not only reduce the burden of exposure at the peak but also shorten the duration of elevated risk, thereby lessening long-term public health pressure.

c. Graph Of Comparation Infected Compartment

In the I(t) compartment, a curative medical intervention control $u_1(t)$ is applied. The following presents a numerical simulation for the I(t) compartment with and without control.

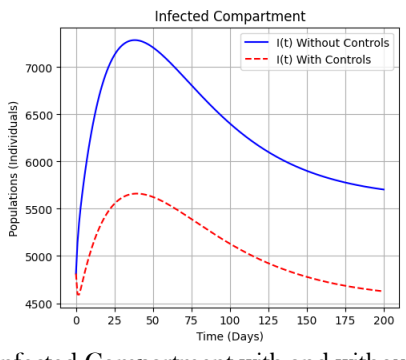


Figure 6. Infected Compartment with and without Controls

The graph in figure 6 compares the trajectory of infected individuals I(t) with and without control measures. In the absence of interventions (blue line), the number of infected individuals rises steeply, peaking at over 7,200 before gradually decreasing. This indicates that uncontrolled transmission sustains a higher disease burden for a longer period. With control measures in place (red dashed line), the peak of infections is significantly lower (around 5,700) and occurs earlier, followed by a sharper decline, the decrease is approximately 20,8%. This pattern shows that interventions not only suppress the peak but also accelerate the reduction of infections, thereby reducing the overall pressure on healthcare systems and mitigating long-term risks.

d. Graph Of Comparation Hospitalized Compartment

In the H(t) compartment, a curative medical intervention control $u_1(t)$ is applied. The following presents a numerical simulation for the H(t) compartment with and without control.

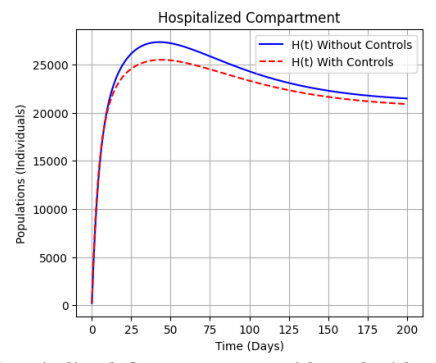


Figure 7. Hospitalized Compartment with and without Controls

Figure 7 depicts the dynamics of hospitalized individuals H(t) under two scenarios: with and without curative medical interventions. In the absence of control, the number of hospitalized patients rises sharply before gradually declining. When curative interventions are applied, the peak is reduced and the subsequent decline is steeper, the decrease is approximately 7,4%. This indicates that timely medical treatment, such as pharmacotherapy, surgical procedures, and intensive hospital-based care, not only prevents further deterioration but also accelerates patient recovery. From a healthcare perspective, curative interventions reduce hospitalization duration and intensity, improving survival and resource efficiency in managing cardiovascular disease.

Numerical Simulation of Cost Function

This cost function (2.3) reflects the trade-off between reducing the number of cases and incurring high expenses for control. The graph of cost function for each control $u_1(t)$, $u_2(t)$, $u_3(t)$ at t = 0 - 80 as follows,

Figure 8. Cost Controls u_1, u_2, u_3 and Comparison Of The Cost Function

The graph in figure 8, illustrates the total costs incurred in reducing cardiovascular disease cases and implementing control measures. During the initial period, expenditures are predominantly allocated to control u_1 , which requires relatively high costs at the outset. In the long term, however, the costs shift toward controls u_2 and u_3 , which are lower in magnitude but sustained over time. Then the next figure illustrates how the total cost evolves under single, combined, and without control strategies for cardiovascular disease management. At the beginning, overall approaches show relatively high cost, reflecting the initial effort required before interventions take effect. Over time, the combined control curve declines more sharply, showing that integrating curative treatment, lifestyle modification, and health education works together to reduce disease progression and related expenses. The total cost under combined control becomes 28,5% lower than that of single control and becomes 86% lower than without control. This finding emphasizes that while comprehensive strategies may require a slightly higher investment at the start, they lead to greater long-term savings and more sustainable health outcomes.

4. CONCLUSION

Based on the findings of this study, a dynamic model of cardiovascular disease was developed by incorporating three control variables. The model was adapted from the SEIR framework in epidemiology. Through this development, the equilibrium points were determined and the global stability of the system was analyzed. Subsequently, optimal control strategies were implemented, and solutions were obtained using Pontryagin's Maximum Principle, which effectively reduced the number of individuals affected by cardiovascular disease. Overall, the integration of the three controls yields an optimal prevention and mitigation strategy: curative control is applied in the initial phase to rapidly reduce the case burden, while lifestyle modification and preventive education maintain a sustained reduction in cases over the long term. After applied the control strategies, we get the reduction of exposed, infected and hospitalized compartment up to 10%, 20,8%, and 7,4%. Then, the susceptible compartment increased up to This approach supports public health policies that combine medical interventions, behavioral changes, and community education as core strategies for controlling cardiovascular disease.

This analysis demonstrates that implementing a combination of control strategies—including curative interventions, lifestyle modification through physical activity, and screening-education programs—yields a more cost-effective outcome compared to applying a single control approach. Quantitatively, the combined control strategy achieves a 28.5% cost reduction relative to the single-control strategy. Furthermore, over a 20-year horizon, the combined approach can reduce the total cost of cardiovascular disease management by up to 86% compared to the no-control scenario. These findings highlight that an integrated control framework not only enhances economic efficiency but also contributes to long-term improvements in population health outcomes.

In conclusion, the control strategy that integrates curative, preventive, and educational components proves to be more effective in reducing both the economic burden and disease prevalence of cardiovascular conditions. Nevertheless, further studies are needed to evaluate the applicability of this model across diverse demographic settings and healthcare systems, ensuring its adaptability and relevance for real-world implementation.

ACKNOWLEDGEMENTS

This research is fully supported by the Research Grant of the Directorate of Research and Community Service, Ministry of Higher Education, Science, and Technology of the Republic of Indonesia under Contract Numbers 077/LL6/PL/AL.04/2025 and A.1/2/062010/LPPM/V/2025.

5. REFERENCES

- [1] S. Cacace and A. Oliviero, "Reliable optimal controls for SEIR models in epidemiology," *Math. Comput. Simul.*, vol. 223, pp. 523–542, 2024, doi: 10.1016/j.matcom.2024.04.034.
- [2] A. F. Akadji, K. A. Mamonto, A. F. D. Hubu, and M. S. Ismail, "Model epidemik SEIR pada kasus penyakit jantung koroner pada penderita kolestrol," *Euler J. Ilm. Mat. Sains dan Teknol.*, vol. 8, no. 1, pp. 1–8, 2020, doi: 10.34312/euler.v8i1.10349.
- [3] S. A. Rezkita, A. M. Pratiwi, and R. Yudhastuti, "The relationship between the effect of obesity and smoking on the incidence of hypertension in the elderly age," *Media Gizi Kesmas*, vol. 12, no. 2, pp. 613–618, 2023, doi: 10.20473/mgk.v12i2.2023.613-618.
- [4] MVP Health Care, "Chapter 9 Hypertension," in *Diseases of the Circulatory System*, 2020, pp. 100–199. doi: 10.2307/j.ctt1hd185t.14.
- [5] G. A. Mensah, G. A. Roth, and V. Fuster, "The global burden of cardiovascular diseases and risk factors: 2020 and beyond," J. Am. Coll. Cardiol., vol. 74, no. 20, pp. 2529–2532, 2019, doi: 10.1016/j.jacc.2019.10.009.
- [6] S. Nurazizah, A. Sani, K. Djafar, W. Somayasa, and L. Gubu, "Model matematika SEIR pada penyakit diabetes mellitus tipe 2," J. Mat. Komputasi dan Stat., vol. 4, no. 1, pp. 523–530, 2024, doi: 10.33772/jmks.v4i1.83.
- [7] L. Jibril and O. Odetunde, "Mathematical modeling and optimal control analysis on sedentary behavior and physical activity in relation to cardiovascular disease (CVD)," *Biomed. Stat. Informatics*, vol. 5, no. 4, pp. 87–99, 2020, doi: 10.11648/j.bsi.20200504.13.
- [8] I. A. Shiddiqie, M. S. Khumaeroh, D. Zulkarnaen, and A. F. Diana, "SEIHR-SEI mathematical model of Zika virus transmission with vector control," *Kubik*, vol. 9, no. 2, pp. 145–160, 2024.
- [9] Nurannisa, R. Ratianingsih, and J. W. Puspita, "Kendali optimal model prognosis sindrom metabolik dengan faktor resiko obesitas dan diabetes melitus tipe II menggunakan Minimum Pontryagin," *J. Ilm. Mat. dan Terap.*, vol. 16, no. 2, pp. 144–157, 2019, doi: 10.22487/2540766x.2019.v16.i2.14990.
- [10] A. U. Samsir, S. Toaha, and Kasbawati, "Optimal control of a mathematical model of smoking with temporary quitters and permanent quitters," *J. Mat. Stat. dan Komputasi*, vol. 18, no. 1, pp. 42–54, 2021, doi: 10.20956/j.v18i1.13974.
- [11] A. Santoso *et al.*, "Towards integrated cardiovascular and mental health management in primary health care in Indonesia: a policy outlook," *Lancet Reg. Heal. Southeast Asia*, vol. 37, no. 100605, pp. 1–10, 2025, doi: 10.1016/j.lansea.2025.100605.
- [12] A. A. Zainuddin et al., "The major risk factor of stroke across Indonesia; a nationwide geospatial analysis of universal health coverage program," Arch. Public Heal., vol. 83, no. 1, 2025, doi: 10.1186/s13690-025-01613-
- [13] J. Y. Lee *et al.*, "Long-term cardiovascular events in hypertensive patients: full report of the Korean Hypertension Cohort," *Korean J. Intern. Med.*, vol. 38, no. 1, pp. 56–67, 2023, doi: 10.3904/kjim.2022.249.
- [14] World Health Organization, "Decade of Healthy Ageing 2021–2030. [Online]. Available [https://www.who.intinitiativesdecade-of-healthy-ageing. Accessed Aug. 17, 2025]."
- [15] E. S. Darmawan, S. R. Hasibuan, V. Y. Permanasari, and D. Kusuma, "Disparities in health services and outcomes by National Health Insurance membership type for ischemic heart disease and stroke in Indonesia: analysis of claims, 2017–2022," Glob. Heal. Res. Policy, vol. 10, no. 1, 2025, doi: 10.1186/s41256-025-00432-v.
- [16] F. R. Muharram et al., "The 30 years of shifting in The Indonesian cardiovascular burden—analysis of the global burden of disease study," J. Epidemiol. Glob. Health, vol. 14, no. 1, pp. 193–212, 2024, doi: 10.1007/s44197-024-00187-8.
- [17] B. Dwiputra *et al.*, "Risk estimation for recurrent cardiovascular events using the SMART-REACH model and direct inpatient cost profiling in Indonesian ASCVD patients: a large-scale multicenter study," *Front. Cardiovasc. Med.*, vol. 11, no. August, pp. 1–9, 2024, doi: 10.3389/fcvm.2024.1425703.
- [18] W. Frąk, A. Wojtasińska, W. Lisińska, E. Młynarska, B. Franczyk, and J. Rysz, "Pathophysiology of cardiovascular diseases: new insights into molecular mechanisms of atherosclerosis, arterial hypertension, and coronary artery disease," *Biomedicines*, vol. 10, no. 8, 2022, doi: 10.3390/biomedicines10081938.
- [19] Dinas Pemberdayaan Masyarakat Desa Kependudukan dan Pencatatan Sipil Provinsi Jawa Tengah, *Profil Perkembangan Kependudukan tahun 2019.* 2020. [Online]. Available: file:///Users/macbook/Downloads/547-Article Text-2022-1-10-20200417.pd
- [20] Bidang Integrasi Pengolahan dan Diseminasi Statistik, Provinsi Jawa Tengah Dalam Angka 2020. Semarang, 2020.
- [21] Dinas Pemberdayaan Masyarakat Desa Kependudukan dan Pencatatan Sipil, *Profil 2021 Perkembangan Kependudukan Provinsi Jawa Tengah*. Semarang, 2022.
- [22] Tim penyusunan Provinsi Jawa Tengah Dalam Angka 2022, *Provinsi Jawa Tengah dalam Angka 2022*. Semarang: CV. Surya Lestari, 2022.

- [23] Dinas Pemberdayaan Masyarakat Desa Kependudukan dan Pencatatan Sipil, Profil Perkembangan Kependudukan 2023 Provinsi Jawa Tengah. Semarang, 2024.
- [24] BPS Provinsi Jawa Tengah, Provinsi Jawa Tengah dalam Angka 2024. Semarang, 2024.
- [25] L. R. Putri, M. Azam, A. A. Nisa, A. I. Fibriana, P. Kanthawee, and S. A. Shabbir, "Prevalence and risk factors of hypertension among young adults: an Indonesian basic health survey," *Open Public Health J.*, vol. 18, 2025, doi: 10.2174/0118749445361291241129094132.
- [26] A. F. Diana, W. Widowati, R. H. Tjahjana, and E. Triyana, "Stability analysis of dynamical model interactions of tea plants, pests, and diseases with fungicide and insecticide controls," *Int. J. Math. Comput. Res.*, vol. 11, no. 01, pp. 3209–3219, 2023, doi: 10.47191/ijmcr/v11i1.14.
- [27] M. I. Widiaputra, A. H. Asyhar, W. D. Utami, P. K. Intan, D. Yuliati, and M. F. Rozi, "Optimal control using Pontryagin's maximum principle: tuberculosis spread case," *Int. J. Comput. Sci. Appl. Math.*, vol. 10, no. 2, 2024, doi: 10.12962/j24775401.v10i2.21958.
- [28] M. Wilhelm *et al.*, "EAPC core curriculum for preventive cardiology," *Eur. Soc. Cardiol.*, vol. 29, pp. 251–274, 2022, doi: 10.1093/eurjpc/zwab017.
- [29] Fatmawati, C. W. Chukwu, R. T. Alqahtani, C. Alfiniyah, F. F. Herdicho, and Tasmi, "A Pontryagin's maximum principle and optimal control model with cost-effectiveness analysis of the COVID-19 epidemic," *Decis. Anal. J.*, vol. 8, no. 100273, 2023, doi: 10.1016/j.dajour.2023.100273.
- [30] S. Nana-Kyere et al., "Global analysis and optimal control model of COVID-19," Comput. Math. Methods Med., vol. 2022, 2022, doi: 10.1155/2022/9491847.
- [31] A. Ramponi and M. E. Tessitore, "Optimal social and vaccination entrol in the SVIR epidemic model," *Mathematics*, vol. 12, no. 993, 2024, doi: 10.3390/math12070933.
- [32] Y. Hu, H. Wang, and S. Jiang, "Analysis and optimal control of a two-strain SEIR epidemic model with saturated treatment rate," *Mathematics*, vol. 12, no. 3026, 2024, doi: 10.3390/math12193026.
- [33] A. Lovison and F. Cardin, "A Pareto Pontryagin maximum Principle for optimal control," *Symmetry (Basel).*, vol. 14, no. 1169, 2022, doi: /10.3390/sym14061169.
- [34] I. K. H. Hermawan, K. C. Kawilarang, and F. Hartono, "Clinical characteristics and profile of heart failure patients at dr. Ramelan Navy Hospital ini 2020," *Cardiovasc. Cardiometabolic Journa*, vol. 1, pp. 9–14, 2022, doi: 10.2473/ccj.v3i1.2022.9-14.
- [35] E. Astutik, S. I. Puspikawati, D. M. S. K. Dewi, A. M. Mandagi, and S. K. Sebayang, "Prevalence and risk factors of high blood pressure among adults in Banyuwangi coastal communities, Indonesia," *Ethiop. J. Health Sci.*, vol. 30, no. 6, pp. 941–950, 2020, doi: 10.4314/ejhs.v30i6.12.
- [36] D. W. Soeatmadji, R. Rosandi, M. R. Saraswati, R. P. Sibarani, and W. O. Tarigan, "Clinicodemographic profile and outcomes of type 2 diabetes mellitus in the Indonesian cohort of discover: A 3-year prospective cohort study," J. ASEAN Fed. Endocr. Soc., vol. 38, no. 1, pp. 68–74, 2023, doi: 10.15605/jafes.038.01.10.
- [37] World Health Organization; The World Bank, "Cardiovascular health at a glance," 2003. [Online]. Available: http://hdl.handle.net/10986/9744